Active Control of Propeller-Induced Noise Fields Inside a Flexible Cylinder

Harold C. Lester*
NASA Langley Research Center, Hampton, Virginia
and
Chris R. Fuller†
Virginia Polytechnic Institute and State University, Blacksburg, Virginia

An active noise control model for reducing aircraft interior noise has been evaluated. The structural noise transmission properties of an aircraft fuselage were modeled as a flexible cylinder excited by external acoustic dipoles simulating the noise produced by twin propellers. The amplitudes of an internal distribution of monopole control sources were determined such that the area-weighted, mean-square acoustic pressure was minimized in the propeller plane. The noise control model was evaluated at low frequencies corresponding to the blade passage frequency and the first few harmonics of a typical turboprop aircraft. Interior noise reductions up to 20 dB were achieved over a substantial region of the cylindrical cross section, with just a few monopole control sources.

Nomenclature

a = radius of cylinder
C_f = speed of sound in air
C_L = axial phase speed in cylinder
E = modulus of elasticity of cylinder
h = cylinder thickness
H_n = complex Hankel function of order n
j = $(-1)^{1/2}$
J_n = complex Bessel function of 1st kind and order n
k = free-space wave number, $k = \omega/C_f$
k_n = axial wave number of nth circumferential cylinder mode
k_n^r = radial wave number of nth circumferential cylinder mode
n = circumferential wave number, $n = 1,2,\ldots,N$
N_c = number of internal monopole control sources
N_s = number of exterior monopole sources
p = acoustic pressure in cylinder
P_α = complex control source amplitudes
S_β = complex amplitudes of exterior monopole sources
t = time, an $e^{-j\omega t}$ time dependence is assumed
x,r,θ = cylindrical coordinates
Y_n = complex Bessel function of the 2nd kind and order n
β = cylinder thickness parameter
ϵ_n = constant, = 1 if $n = 0$, otherwise, = 2
Λ,Λ_0 = cost functions
ν = Poisson's ratio
ρ_f = density of air
ρ_s = density of cylinder
$\Phi_{n\beta}$ = modal distribution functions
$\Psi_{n\alpha}$ = modal distribution functions
Ω = nondimensional frequency, $= \omega a/C_L$
ω = steady-state circular frequency

Superscripts
T = matrix or vector transpose
$*$ = complex conjugate

Received July 15, 1987; revision received Aug. 25, 1989.

*Aerospace Engineer, Structural Acoustics Branch.
†Professor, Mechanical Engineering. Member AIAA.

Introduction

THE evolution of advanced turboprop aircraft has spawned an increase in active noise control research. These aircraft offer significant increases in fuel efficiency over conventional fanjets. However, because of higher blade-tip speeds, advanced turboprop propulsion systems will produce considerably higher interior noise levels. To reduce these higher interior noise levels by purely conventional passive methods may be both inefficient and uneconomical, hence the growing interest in developing applicable active noise control technology.

Although the fundamental concepts associated with active noise control are not new,[1] the aircraft interior noise application is relatively recent. The 1984 paper by Zalas and Tichy[2] demonstrated that a single acoustic driver could produce substantial interior noise reductions at blade passage harmonics, although the spatial effect was highly localized. Research by Fuller[3] has added considerably to the understanding of transmission phenomena associated with infinitely long, elastic cylinder models excited by internal and external acoustic monopole sources. Fuller also investigated reducing interior noise of propeller aircraft by means of synchrophasing.[4]

In this paper an evaluation is made of an active noise control concept for reducing propeller-induced aircraft interior noise. The structural properties of an aircraft fuselage are modeled as an infinitely long, thin, elastic cylinder.[3-6] The primary acoustic field inside the cylinder is assumed to be produced by the dynamic response of the shell to harmonic acoustic dipoles. These dipoles are located outside the cylinder and approximate the noise produced by propellers.[4] The source strengths (amplitude and phase) and locations of the dipoles are specified a priori. Hence, the primary acoustic field is assumed to be known.

A control field is produced inside the flexible cylinder by a distribution of acoustic monopole sources.[6] The complex source strengths (amplitude and phase) of these control sources are determined such that the area-weighted, mean-square pressure is a minimum in the source (propeller) plane. This approach leads to a linear matrix equation for the unknown source strengths.[7] Therefore, the essence of this active noise control model centers on finding a control field such that

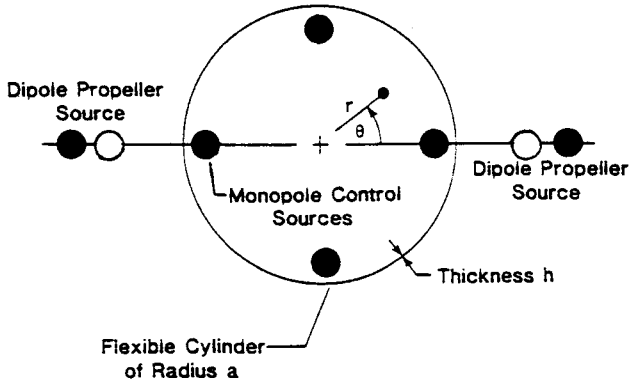

Fig. 1 Aircraft fuselage/propeller model with acoustic control sources.

the composite (primary plus control) field is less than the original primary field.

Analysis

Essential elements of the aircraft fuselage/propeller model are shown in Fig. 1. Structurally the fuselage is represented as an infinitely long, thin, flexible cylinder of radius a and uniform thickness h. The cylinder displacements are described by a classical thin shell theory which neglects the effects of transverse shear and rotary inertia.[4-6,8]

Instead of the axial resonance characteristics associated with a finite-length cylinder having rigid-end caps, the wave theory used for the infinitely long cylinder displays the well known cut-on phenomena for the shell and cavity modes. In addition, with the wave theory the coupling between the cylinder and the interior and exterior acoustic responses is retained, although these radiation damping effects are expected to be small for the light loading afforded by an air medium. It thus seems reasonable to assume that the wave theory will provide some insight into the basic coupling mechanisms occurring between the cylinder and interior acoustic cavity response.

The primary acoustic pressure field inside the cylinder is assumed to be produced by the dynamic response of the shell to two external acoustic dipoles. This pair of dipoles is used to simulate the external sound field produced by twin propellers. As illustrated in Fig. 1, each propeller dipole is approximated as a pair of closely spaced acoustic monopoles.[4] The complex amplitudes (amplitude and phase) and locations of the dipole sources are specified a priori. Hence, the interior acoustic field, produced by the propeller sources, is assumed to be known in the following analysis. This acoustic field will be referred to throughout this paper as the primary acoustic field and will be defined in the following section.

Also shown in Fig. 1 are the interior acoustic monopoles used as the noise reduction elements of the active noise control model. The number and location of the interior control sources are variables, although all of the control sources will be located the same radial distance from the inside shell wall. The interior acoustic field, produced by the assumed distribution of monopole control sources, will hereafter be referred to as the control field. The purpose of this active noise control study is to determine the control field such that the combined primary and control field is less than the original primary acoustic field.

Primary Acoustic Field

The steady-state acoustic field produced inside the flexible cylinder by the external dipoles can be represented as[4] (see also the Appendix)

$$p_p(r,\theta) = \sum_{\beta=1}^{N_s} S_\beta B_\beta(r,\theta,r_\beta,\phi_\beta) \tag{1}$$

where four monopoles (located at r_β, ϕ_β) are required to represent the two dipole propeller sources, hence $N_s = 4$. The distribution functions $B_\beta\ (r,\theta,r_\beta,\phi_\beta)$ appearing in Eq. (1) are given by

$$B_\beta\ (r,\theta,r_\beta,\phi_\beta) = \sum_{n=0}^{N} \Phi_{n\beta}(r,r_\beta)\cos[n(\theta-\phi_\beta)] \tag{2}$$

where [see Eq. (A11)]

$$\Phi_{n\beta}(r,r_\beta) = \left(\frac{\epsilon_n\Omega^2}{\pi a}\right)\left(\frac{\rho_f}{\rho_s}\right)\left(\frac{a}{h}\right)I_n^{(3)}(x,r,r_\beta) \tag{3}$$

Thus, in Eq. (2), $\Phi_{n\beta}(r,r_\beta)$ is the distribution for the acoustic pressure in the nth circumferential mode. The modal response integrals $I_n^{(3)}(x,r,r_\beta)$ are defined in Table 1. Details of their derivation are given by Fuller[4-6] and are outlined in the Appendix. The nondimensional frequency parameter Ω is

$$\Omega = \frac{\omega a}{C_L} \tag{4a}$$

where ω is the source frequency and C_L is the phase speed of axial propagating waves in the cylinder. In terms of the nondimensional frequency parameter ka commonly used for duct modes,

$$\Omega = ka\left(\frac{C_f}{C_L}\right) \tag{4b}$$

Returning to Eq. (1), S_β denotes the complex amplitudes of the four external monopoles sources used to model the propeller noise. These sources were located as follows

$$\frac{r_\beta}{a} = (2,\ 2.2,\ 2,\ 2.2) \tag{5a}$$

$$\phi_\beta = (0,\ 0,\ \pi,\ \pi) \tag{5b}$$

where $\beta = 1, 2, 3, 4$. Since linear acoustics is assumed, the magnitudes of the source strengths were set to unity, that is,

$$|S_\beta| = 1 \tag{5c}$$

leaving the phase angles of S_β as variables in order to account for propeller phasing effects.[4]

Control Field

In a similar manner, the steady-state noise field produced inside the cylinder by a distribution of interior monopole sources (see Fig. 1) can be expressed as

$$p_s(r,\theta) = \sum_{\alpha=1}^{N_c} P_\alpha A_\alpha(r,\theta,r_\alpha,\theta_\alpha) \tag{6}$$

where

$$A_\alpha\ (r,\theta,r_\alpha,\theta_\alpha) = \sum_{n=0}^{N} \Psi_{n\alpha}(r,r_\alpha)\cos[n(\theta-\theta_\alpha)] \tag{7}$$

Four interior monopole control sources are indicated in Fig. 1, although the actual number and location of the sources varied from case to case. For the results presented in this paper, all control sources were located at the same radial coordinate

$$r_\alpha = 0.875a \tag{8}$$

where $\alpha = 1, 2, \ldots, N_c$. As with the primary field, the control field [(Eqs. (6) and (7)] is represented as a superposition of $n = 1, 2, \ldots, N$ circumferential modes with $\Psi_{n\alpha}\ (r,r_\alpha)$ being the corresponding distribution function for the nth mode. This function is given by[5,6] [(see Eq. (A2)]

$$\Psi_{n\alpha}(r,r_\alpha) = \frac{\epsilon_n}{a}\left(\frac{2\Omega^2}{\pi}\right)\left(\frac{\rho_f}{\rho_s}\right)\left(\frac{a}{h}\right)[I_n^{(1)}(x,r,r_\alpha) + I_n^{(2)}(x,r,r_\alpha)] \tag{9}$$

The modal response integrals, $I_n^{(1)}(x,r,r_\alpha)$ and $I_n^{(2)}(x,r,r_\alpha)$, are defined in Table 1.

Table 1 Modal response integrals

$$I_n^{(1)}(x,r,r_0) = \int_{-\infty}^{+\infty}\left[\frac{J_n(k_n^r r_0)}{k_n^r a J_n(k_n^r a)}\right]\left[\frac{J_n(k_n^r r)}{k_n^r a J_n(k_n^r a)}\right] I_{33}\exp\left[j(k_n a)\left(\frac{x}{a}\right)\right]\mathrm{d}(k_n a)$$

$$I_n^{(2)}(x,r,r_0) = \begin{cases} \displaystyle\int_{-\infty}^{+\infty}\left[\frac{J_n(k_n^r r_0)}{J_n(k_n^r a)}\right][J_n(k_n^r r)Y_n'(k_n^r a) - J_n'(k_n^r a)Y_n(k_n^r r)] \\ \quad \times \exp\left[j(k_n a)\left(\frac{x}{a}\right)\right]\mathrm{d}(k_n a) & \text{for } r > r_0 \\ \displaystyle\int_{-\infty}^{+\infty}\left[\frac{J_n(k_n^r r)}{J_n'(k_n^r a)}\right][J_n(k_n^r r_0)Y_n'(k_n^r a) - J_n'(k_n^r a)Y_n(k_n^r r_0)] \\ \quad \times \exp\left[j(k_n a)\left(\frac{x}{a}\right)\right]\mathrm{d}(k_n a) & \text{for } r < r_0 \end{cases}$$

$$I_n^{(3)}(x,r,r_0) = \int_{-\infty}^{+\infty}\left[\frac{H_n(k_n^r r_0)}{k_n^r a H_n'(k_n^r a)}\right]\left[\frac{J_n(k_n^r r)}{k_n^r a J_n'(k_n^r a)}\right] I_{33}\exp\left[j(k_n a)\left(\frac{x}{a}\right)\right]\mathrm{d}(k_n a)$$

The complex amplitudes P_α appearing in Eq. (6) are not known in advance. These quantities must be determined such that the propeller-induced noise (primary field) inside the cylinder is reduced in some sense. A minimization procedure for accomplishing this is developed in the following sections.

Cost Function

The total steady-state acoustic field inside the cylinder is obtained by adding Eqs. (1) and (6)

$$p(r,\theta) = \sum_{\alpha=1}^{N_c} P_\alpha A_\alpha(r,\theta,r_\alpha,\theta_\alpha) + \sum_{\beta=1}^{N_s} S_\beta B_\beta(r,\theta,r_\beta,\phi_\beta) \tag{10}$$

The second term on the right side of Eq. (10) is due to the known primary field produced by the external dipole (propeller) sources. The first term is due to the control field. Here the number N_c and location (r_α,θ_α) of the interior monopoles must be specified and the amplitudes P_α determined to reduce the overall interior noise level in the cylinder.

In this paper, the amplitudes P_α of the control sources are determined such that the area-weighted, mean-square pressure Λ is a minimum. Thus, the cost function is

$$\Lambda(P_\alpha) = \frac{1}{A_0}\int_0^a\int_0^{2\pi} |p(r,\theta)|^2 r\,\mathrm{d}r\,\mathrm{d}\theta \tag{11}$$

where $p(r,\theta)$ is given by Eq. (10) and $A_0 = \pi a^2$. An explicit dependence of Λ is indicated with respect to the complex control source amplitudes P_α ($\alpha = 1,2,\ldots,N_c$) since these variables will be determined such that Λ, as given by Eq. (11), is a minimum.

Substituting Eq. (10) into Eq. (11) and performing the integrations allows the cost function to be expressed as

$$\Lambda(\bar{P}) = \bar{P}^T[A]\bar{P}^* + \bar{S}^T[B]\bar{P}^* + \bar{P}^T[B^*]^T\bar{S}^* + \bar{S}^T[C]\bar{S}^* \tag{12}$$

where

$$\bar{P}^T = [P_1,P_2,\ldots,P_{N_c}] \tag{13}$$

$$\bar{S}^T = [S_1,S_2,\ldots,S_{N_s}] \tag{14}$$

Thus, Eq. (12) expresses the cost function Λ as a real, homogeneous, quadratic function of the complex amplitudes $P_1,P_2,\ldots,P_{N_c}$.

The matrices appearing in Eq. (12) have the following forms:

$$[A] = \frac{1}{A_0}\int_0^a\int_0^{2\pi}[\bar{A}\bar{A}^{*T}]\,r\,\mathrm{d}r\,\mathrm{d}\theta \tag{15}$$

$$[B] = \frac{1}{A_0}\int_0^a\int_0^{2\pi}[\bar{B}\bar{A}^{*T}]\,r\,\mathrm{d}r\,\mathrm{d}\theta \tag{16}$$

$$[C] = \frac{1}{A_0}\int_0^a\int_0^{2\pi}[\bar{B}\bar{B}^{*T}]\,r\,\mathrm{d}r\,\mathrm{d}\theta \tag{17}$$

where the elements of the vector $\bar{A}$ are

$$\bar{A}^T = [A_1,A_2,\ldots,A_{N_c}] \tag{18}$$

and are defined by Eq. (7) and the elements of the $\bar{B}$ vector are

$$\bar{B}^T = [B_1,B_2,\ldots,B_{N_s}] \tag{19}$$

and are defined by Eq. (2).

A typical element in the ith row and jth column of the square $[A]$ matrix ($i,j = 1,2,\ldots,N_c$) has the form

$$A_{i,j} = \frac{\pi}{A_0}\sum_{n=0}^{N}\epsilon_n C_{nij}\cos[n(\theta_{\alpha_i} - \theta_{\alpha_j})] \tag{20}$$

where

$$C_{nij} = \int_0^a \Psi_{n\alpha_i}(r,r_{\alpha_i})\Psi_{n\alpha_j}^*(r,r_{\alpha_j})r\,\mathrm{d}r \tag{21}$$

In Eq. (20), the θ_{α_i} ($\alpha_1,\alpha_2,\ldots,\alpha_{N_c}$) are the azimuthal locations of the N_c interior monopole control sources. Similarly, a typical term in the ith row ($i = 1,2,\ldots,N_s$) and jth column ($j = 1,2,\ldots,N_c$) of the $[B]$ matrix has the form

$$B_{i,j} = \frac{\pi}{A_0}\sum_{n=0}^{N}\epsilon_n B_{nij}\cos[n(\phi_{\beta_i} - \phi_{\alpha_j})] \tag{22}$$

where

$$B_{nij} = \int_0^a \Phi_{n\beta_i}(r,r_{\beta_i})\Psi_{n\alpha_j}^*(r,r_{\alpha_j})r\,\mathrm{d}r \tag{23}$$

The fourth term appearing in Eq. (12) is a scalar constant since the elements of $\bar{S}$ are assumed known. This term does not affect the optimal solution of Eq. (12). It can most easily be neglected by defining a shifted cost function Λ_0 where

$$\Lambda_0(\bar{P}) = \Lambda(\bar{P}) - \bar{S}^T[C]\bar{S}^* \tag{24}$$

or finally

$$\Lambda_0(\bar{P}) = \bar{P}^T[A]\bar{P}^* + \bar{S}^T[B]\bar{P}^* + \bar{P}^T[B^*]^T\bar{S}^* \tag{25}$$

Table 2 Modal response characteristics

	Cut-on frequency Ω_n		
n	Acoustic modes $(n, 0)$	$(n, 1)$	Cylinder modes (Class I)[10]
0	0.0	0.242	
1	0.116	0.337	0.0
2	0.193	0.424	0.007
3	0.265	0.506	0.020
4	0.336	0.586	0.040
5	0.405	0.665	0.068
6	0.474	0.741	0.100
7	0.542	0.817	0.137
8	0.609	0.892	0.180
9	0.667	0.966	0.223

Optimal Solution

A solution $\bar{P}$ is sought for Eq. (25) such that the cost function $\Lambda_0(\bar{P})$ is a minimum. The $\bar{P}$ vector, for which $\Lambda_0(\bar{P})$ takes a minimum value, can be obtained by differentiating Eq. (25) with respect to the real and imaginary parts of $\bar{P}$ and setting the resulting equations to zero.[7] Furthermore, since $[A]$ is a symmetric, positive definite matrix, the cost function will possess a unique global minimum. The optimal solution is

$$\bar{P} = -[A]^{-1}[B]^T\bar{S} \tag{26}$$

In the following, Eq. (26) will be used to calculate the control source complex amplitudes (amplitude and phase) for several primary fields and control source distributions.

Discussion of Results

Before several illustrative examples of this active noise control model are presented and discussed, it will be useful to describe some of the physical properties and basic response characteristics of the system.

Configuration Response Characteristics

Physical properties of the active noise control model are typical of standard aluminum and air at 20°C. The cylinder has a radius of 0.4 m and a thickness of 0.001 m giving a thickness-to-radius ratio of 0.0025. To numerically evaluate the response integrals appearing in Table 1, it was necessary to introduce damping into the fluid medium by replacing the velocity of sound C_f in these integrals by

$$C_f = 343.0\,(1 - j\eta_f) \tag{27}$$

In a similar manner, damping was added to the shell material by replacing the modulus of elasticity E by $(1 - j\eta_s)\,E$. However, since the axial phase speed C_L is proportional to $(E)^{1/2}$, this effectively gives

$$C_L = 5432.0\,(1 - j\eta_s)^{1/2} \tag{28}$$

Values of $\eta_f = 0.001$ and 0.02 were found to be small enough such that the response integrals could be evaluated numerically and still leave the overall system response essentially undamped.

In Table 2, cut-on frequencies are summarized for the first 10 flexural cylinder modes and the first 10 $(n, 0)$ and $(n, 1)$ acoustic (duct) modes of the cylindrical cross section. The cut-on frequencies Ω_n for the hard-wall duct modes can be calculated using[9]

$$\Omega_n = \frac{C_f}{C_L}\,(\lambda_{n,m}a) \tag{29}$$

where the eigenvalues $\lambda_{n,m}$ are the zeros of

$$J_n'(\lambda_{n,m}a) = 0 \tag{30}$$

A similar interpretation holds for the cut-on frequencies of the cylinder modes (see Table 2). These modes, termed class I flexural shell modes, can couple efficiently with the interior acoustic cavity modes. Cut-on frequencies for these modes can be calculated from an equation by Smith[10] repeated here

$$\Omega_n^2 = \frac{4}{3}\left(\frac{h}{a}\right)^2\left[\frac{n^2(n^2-1)^2}{n^2+1}\right] \tag{31}$$

where $n > 1$. The important point evident in Table 2 is that, at any given frequency, there are more cylinder modes propagating than acoustic duct modes. Thus, for a driving frequency of $\Omega = 0.22$, the $n = 2, 3, 4, 5, 6, 7, 8$ cylinder modes are cut on, whereas only the (0, 0), (0, 1), and (0, 2) duct modes can propagate.

Plane Wave with Out-of-Phase Dipoles

Figure 2 shows a typical result for the active noise control model when the driving frequency is $\Omega = 0.10$. At this fre-

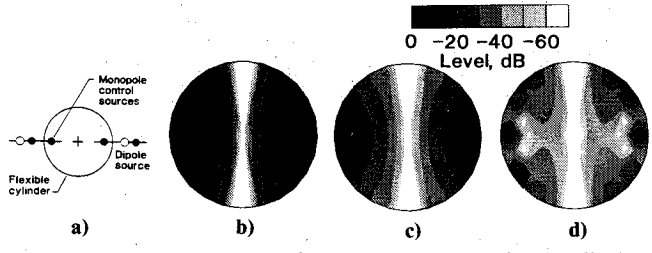

Fig. 2 Interior pressure maps for two external out-of-phase dipoles and two control sources, $\Omega = 0.10$: a) source locations and phasing, b) primary field, c) control field, and d) composite field.

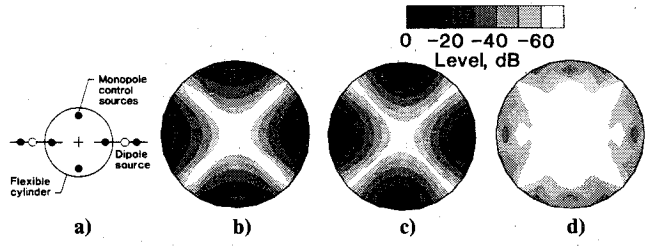

Fig. 3 Interior pressure maps for two external in-phase dipoles and four control sources, $\Omega = 0.10$: a) source locations and phasing, b) primary field, c) control field, and d) composite field.

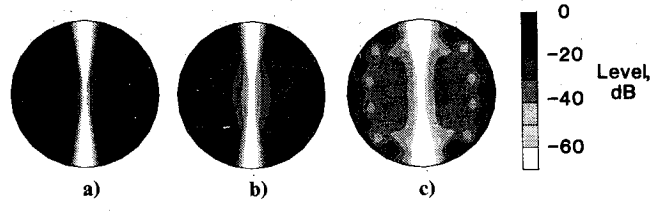

Fig. 4 Interior pressure maps for two control sources configurations, out-of-phase dipoles, $\Omega = 0.15$: a) primary field, b) composite field for two control sources, $\theta_c = 0$ and 180 deg, and c) composite field for six control sources, $\theta_c = 0, 60, \ldots, 300$ deg.

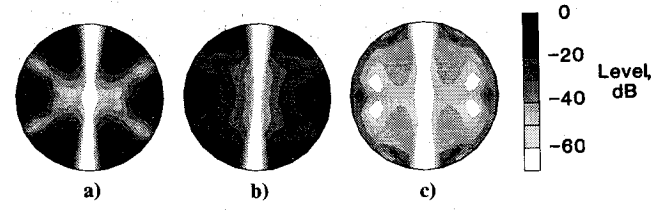

Fig. 5 Interior pressure maps for two control sources configurations, out-of-phase dipoles, $\Omega = 0.22$: a) primary field, b) composite field for two control sources, $\theta_c = 0$ and 180 deg, and c) composite field for six control sources, $\theta_c = 0, 60, \ldots, 300$ deg.

quency, Table 2 indicates that only the $n = 0$ (plane wave) acoustic mode can propagate inside the cylinder, although numerous cylinder modes are cut on. The dipoles are set 180 deg out-of-phase. The phasing of the dipoles is indicated in part a of Fig. 2 by the white/black shading of the component monopoles. It should be noted that, by operating the dipoles out-of-phase, an intense interior noise field is created inside the cylinder. Fuller[4] refers to this as the unsynchrophased case. The primary field is shown mapped in part b of Fig. 2 where the peak pressure level is set to 0 dB as indicated by black on the gray bar scale. The primary field strongly suggests a "forced" $n = 1$ antisymmetric response, although the cylinder responds (not shown) about equally in the $n = 1$ and 3 circumferential modes. The $n = 1$ cylinder mode, therefore, passes energy to the interior more efficiently than does the $n = 3$ cylinder mode.

With two control sources, the active control model produces, by means of Eq. (26), the control field shown in part c of Fig. 2. The control field also displays a predominant $n = 1$ behavior and is thus quite similar to the primary field in magnitude but opposite in-phase (not shown). The composite field (primary plus control) is mapped in part d of Fig. 2. The two interior acoustic control sources therefore produce reduced noise levels of about 15–20 dB over a fairly large region of the cross section.

Plane Wave with In-Phase Dipoles

If, in contrast to the preceding case, the dipoles are driven in-phase, the results are as shown in Fig. 3. The primary field is shown in part b, and in this instance these results are normalized to the peak noise level of part b of Fig. 2. Thus, in comparing the results of part b of Figs. 2 and 3, the additional effects of propeller synchrophasing are exhibited.[4] Note that, with the external dipoles in-phase, the primary acoustic response is in the $n = 2$ circumferential mode. The shell response is also limited to this circumferential mode and thus, with the external dipoles in-phase, the cylinder is forced to respond in a higher order mode with reduced transmission efficiency, and the interior noise levels are much lower.

Since the primary field for this case displays an $n = 2$ character, four acoustic control sources, located at $\theta_c = 0$, 90, 180, and 270 deg, were used in the active noise control model. The actual control field is shown mapped in part c of Fig. 3. Note that all results of part b of Fig. 3 have been normalized to the peak noise level of part b of Fig. 2. The composite of the primary and control fields is presented in part d of Fig. 3. For this case, with the dipoles in-phase, reductions of more than 20–25 dB are obtained over a significant subregion of the cylinder's cross section. This reduction is the combined result of source phasing and the interior control sources.

Two Acoustic Modes with Out-of-Phase Dipoles

Next consider a higher frequency case with $\Omega = 0.15$. At this frequency, Table 2 shows that there are two acoustic modes propagating in the cylinder, whereas the first eight cylinder modes propagate. Results are presented in Fig. 4 for two different control source configurations. Results for this out-of-phase case are very similar to the maps of Fig. 2. The primary field again indicates an $n = 1$ antisymmetric response, although a slight $n = 3$ modal component is present. However, the $n = 1$ cylinder mode couples more readily with the interior acoustical space and most of the energy is transferred to the $n = 1$ acoustic mode.

The composite field produced when two control sources ($\theta_c = 0$ and 180 deg) are employed is shown in part b of Fig. 4. The results show a trace of an $n = 3$ modal component, which is also present in the primary field. The control sources therefore reduce the contribution of the $n = 1$ mode such that the $n = 3$ model component is more visible. This produces a slight reduction in the interior noise. To capitalize on this effect, six control sources, located at $\theta_c = 0$, 60,..., 300 deg, were used in the active noise control model. The results are shown in part c of Fig. 4 and indicate even greater interior noise reductions.

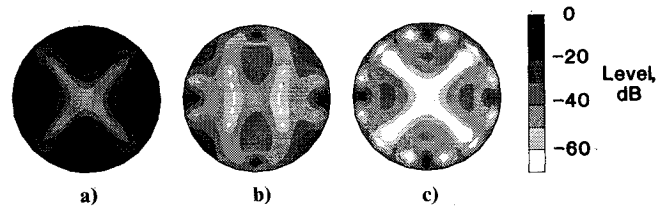

Fig. 6 Interior pressure maps for two control sources configurations, in-phase dipoles, $\Omega = 0.22$: a) primary field, b) composite field for four control sources, $\theta_c = 0, 90,...,270$ deg, and c) composite field for eight control sources, $\theta_c = 0, 45,...,315$ deg.

Three Acoustic Modes with Out-of-Phase Dipoles

At a frequency $\Omega = 0.22$, the $n = 0$, 1, and 2 acoustic modes can propagate in the cylinder (see Table 2). Results with the external dipoles out-of-phase are shown in Fig. 5 for two control source arrangements. Here the primary field shows a much more complicated modal pattern. Significant contributions of the $n = 1$ and $n = 3$ circumferential modes are apparent.

The composite field produced with just two control sources, located at $\theta_c = 0$ and 180 deg, is shown in part b of Fig. 5. In this instance noise reductions up to 20 dB are achieved. Actually, for this case the control field (not shown) shows a strong excitation of the $n = 1$ acoustic mode but only a weak excitation of the $n = 3$ component, which is readily apparent in the primary field (see part a of Fig. 5). That is, in this case the control field does not well replicate the primary field. To create an appreciable response in the $n = 3$ acoustic mode, six interior control sources, located at $\theta_c = 0$, 60,..., 300 deg, were used, and the resulting composite field is shown in part c of Fig. 5. For this arrangement of the interior control sources, the control field (not shown) is again quite similar to the primary field (see part a of Fig. 5). The result is an appreciable increase in the effectiveness of the active noise control system, as indicated by interior noise reductions of more than 20 dB over a much greater region of the cross section as compared with the two control sources case (see part b of Fig. 5).

Three Acoustic Modes with In-Phase Dipoles

Similar results, when the external dipoles are in phase, are presented in Fig. 6. Composite fields are shown in parts b and c for four and eight control sources, respectively. With the dipoles in-phase, the interior acoustic response occurs primarily in the $n = 2$ mode. Both control source arrangements produce appreciable noise reductions of the order of 15–20 dB or more over a substantial region of the source plane.

Concluding Remarks

This paper has sought to evaluate an active noise control concept for reducing propeller-induced aircraft interior noise. The structural properties of an aircraft fuselage were modeled as an infinitely long, elastic cylinder. The primary acoustic field inside the cylinder was produced by the dynamic response of the shell to two external dipoles, which modeled the noise produced by twin propellers. A control field was produced inside the cylinder by a distribution of acoustic monopole sources. The complex strengths of the control sources were determined such that the area-weighted, mean-square acoustic pressure was a minimum over the source (propeller) plane.

The active noise control model was evaluated at low frequencies where interior fuselage noise is typically dominated by the response at the blade passage frequency and first few harmonics. The active noise control model produced reductions of up to 20 dB over a substantial region of the cylindrical cross section. These reductions were achieved with only a few (two to eight) judiciously placed monopole control sources. Apparently, when the primary acoustic field displays an iden-

tifiable response in just a few modes, the minimization algorithm is capable of generating a similar acoustic modal pattern (by means of the acoustic control sources) of opposite phase. The control sources must therefore be located such that this preferred acoustic modal response can be excited. Generally, the number of control sources was dictated by the well known Nyquist criterion. That is, significant interior noise reductions were achieved when the number of control sources equaled twice the circumferential mode order of the highest order offending acoustic mode.

Optimum results were achieved when source phasing was used in combination with active noise control. By varying the phase between the external dipoles, the cylinder can be forced to respond in a mode with reduced transmission properties and/or in a primary field modal pattern that can be more favorably replicated by the interior control source configuration. This suggests that source phasing may be an important variable in an active system for reducing aircraft interior noise.

Appendix: Acoustic Response Equations

This appendix summarizes the response relations necessary for computing the acoustic pressure field produced inside a flexible cylinder by an exterior monopole acoustic noise source or by a similar noise source located inside the cylinder. Only the steady-state ($e^{-j\omega t}$) response is considered, and the cylinder is assumed to be infinitely long. Details of this analysis are developed in Refs. 3-6 and 8.

Interior Source Solution

Consider the shell/monopole configuration depicted in Fig. A1. It is convenient to work in cylindrical coordinates (x,r,θ). The cylinder has a thickness h and a radius a. A monopole acoustic source, with amplitude P_α, is assumed located at $r = r_\alpha$ and $\theta = 0$, where $r_\alpha < a$.

As developed by Fuller,[6] the steady-state acoustic pressure field produced inside the flexible cylinder by this harmonically pulsating monopole is given by

$$p(x,r,\theta) = P_\alpha \sum_{n=0}^{\infty} \Psi_{n\alpha}(r,r_\alpha)\cos(n\theta) \tag{A1}$$

where

$$\Psi_{n\alpha}(r,r_\alpha) = \frac{\epsilon_n}{a}\left(\frac{2\Omega^2}{\pi}\right)\left(\frac{\rho_f}{\rho_s}\right)\left(\frac{a}{h}\right)[I_n^{(1)}(x,r,r_\alpha) + I_n^{(2)}(x,r,r_\alpha)] \tag{A2}$$

The nondimensional frequency parameter Ω is

$$\Omega = \frac{\omega a}{C_L} \tag{A3}$$

where ω is the source driving frequency and C_L is the axial phase speed in the shell. Note that

$$C_L = \left[\frac{E}{\rho_s(1-\nu^2)}\right]^{1/2} \tag{A4}$$

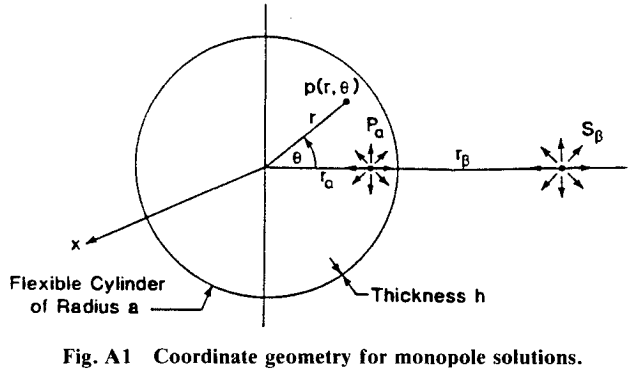

Fig. A1 Coordinate geometry for monopole solutions.

where E and ν are the modulus of elasticity and Poisson's ratio, respectively, of the shell material.

The modal response integrals, $I_n^{(1)}(x,r,r_\alpha)$ and $I_n^{(2)}(x,r,r_\alpha)$, are defined in Table 1 of the main text. The shell response elements L_{ij} are

$$L_{11} = \frac{n^2}{2}(1-\nu) + (k_n a)^2 - \Omega^2$$

$$L_{12} = L_{21} = \frac{n}{2}(1+\nu) + (k_n a)$$

$$L_{13} = L_{31} = \nu(k_n a)$$

$$L_{22} = n^2 + \frac{(1-\nu)}{2(k_n a)^2 - \Omega^2}$$

$$L_{23} = L_{32} = n$$

$$L_{33} = 1 - \Omega^2 + \beta^2[n^2 + (k_n a)^2]^2 - FL \tag{A5}$$

The parameter I_{33} (see Table 1 of the main text) is the (3,3) element of the inverse of $[L]$:

$$I_{33} = \frac{(L_{11}L_{22} - L_{12}L_{21})}{DET(L)} \tag{A6}$$

Also, the thickness parameter β has the definition

$$\beta^2 = \frac{h^2}{12a^2} \tag{A7}$$

The fluid loading term FL, associated with the contained fluid (air) and the coupled external radiation field, is given by the following equation.

$$FL = \Omega^2\left(\frac{a}{h}\right)\left(\frac{\rho_f}{\rho_s}\right)\left[\frac{J_n(k_n^r a)}{(k_n^r a)J_n'(k_n^r a)} - \frac{H_n(k_n^r a)}{(k_n^r a)H_n'(k_n^r a)}\right] \tag{A8}$$

The radial wave number is related to the axial wave number through the equation

$$k_n^r a = \left[\left(\frac{C_L\omega}{C_f}\right)^2 - (k_n a)^2\right]^2 \tag{A9}$$

where C_f is the speed of sound of the surrounding medium.

Exterior Source Solution

Now consider the same situation except that the monopole acoustic source is located outside the cylinder (see Fig. A1) at radial coordinate $r_\beta (r_\beta > a)$. The acoustic pressure field produced inside the cylinder by this external monopole is also derived by Fuller[4] and can be expressed as follows

$$p(x,r,\theta) = S_\beta \sum_{n=0}^{\infty} \Phi_{n\beta}(r,r_\beta)\cos(n\theta) \tag{A10}$$

where

$$\Phi_{n\beta}(r,r_\beta) = \left(\frac{\epsilon_n\Omega^2}{\pi a}\right)\left(\frac{\rho_f}{\rho_s}\right)\left(\frac{a}{h}\right)I_n^{(3)}(x,r,r_\beta) \tag{A11}$$

The modal response integral $I_n^{(3)}(x,r,r_\beta)$ is defined in Table 1 of the main text. The other quantities required by Eqs. (A10) and (A11) are the same as for the interior monopole case [Eqs. (A3) and (A9)].

References

[1]Ffowcs Williams, J. E., Roebuck, I., and Ross, C. F., "Anti-Phase Noise Reduction," *Physics in Technology,* Vol. 16, 1985.

[2]Zalas, J. M., and Tichy, J., "Active Attenuation of Propeller Blade Passage Noise," NASA CR-172386, July 1984.

[3]Fuller, C. R., Mechanisms of Transmission and Control of Low-Frequency Sound in Aircraft Interiors, SAE Technical Paper 850879, April, 1985.

[4]Fuller, C. R., Analytical Investigation of Synchrophasing as a Means of Reducing Aircraft Interior Noise, NASA CR-3823, Aug. 1984.

[5]Fuller, C. R., and Fahy, F. J., "Characteristics of Wave Propagation and Energy Distributions in Cylindrical Elastic Shells Filled with Fluid," *Journal of Sound and Vibration,* Vol. 81, No. 4, 1982, pp. 501-518.

[6]Fuller, C. R., "Radiation of Sound from an Infinite Cylindrical Elastic Shell Excited by an Internal Monopole Source," *Journal of Sound and Vibration,* Vol. 109, No. 2, 1986, pp. 259-275.

[7]Nelson, P. A., and Elliott, S. J., "A Note on the Active Minimization of Steady Enclosed Sound Fields," ISVR Memorandum No. 647, Feb. 1984.

[8]Fahy, F. J., *Sound and Structural Vibration: Radiation, Transmission and Response,* Academic, New York, 1985.

[9]Pierce, A. D., *Acoustics: An Introduction to Its Physical Principles and Applications,* McGraw-Hill, New York, 1981.

[10]Smith, P. W., Jr., "Phase Velocities and Displacement Characteristics of Free Waves in a Thin Cylindrical Shell," *Journal of Acoustical Society of America,* Vol. 27, No. 6, 1955, pp. 1065-1072.